Joint Milli-Arcsecond Pathfinder Survey (JMAPS) Fine Attitude Determination Approach

T.W. Lim, F.A. Tasker, and P.G. DeLaHunt
Spacecraft Engineering Department

Introduction: The Joint Milli-Arcsecond Pathfinder Survey[1] (JMAPS) is a Department of the Navy space astrometry mission to conduct an all-sky, bright star astrometric and spectrophotometric survey. The primary goal of the mission is to update the bright star catalog currently used by Department of Defense, NASA, and commercial star tracker manufacturers for spacecraft attitude determination. Secondary goals include the development and flight demonstration of an advanced detector such as the H4RG-10 CMOS-Hybrid detector/readout sensor. The JMAPS spacecraft configuration and instrument specifications are shown in Fig. 1.

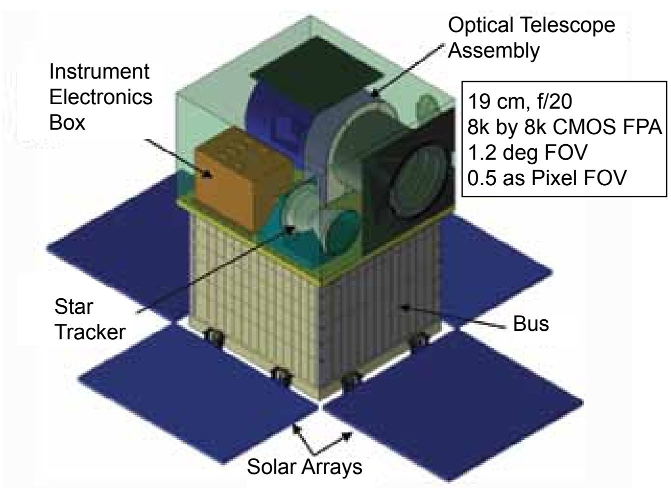

FIGURE 1
JMAPS space vehicle design (from Ref. 1).

To support the mission star catalog accuracy of 1 milli-arcsecond (mas) in position, 1 mas/year in proper motion, and 1 mas in parallax, the instrument line-of-sight must maintain its pointing stability of 50 mas (1 σ) during observation. This stringent requirement is met in part by using the instrument as a fine attitude determination star tracker to produce an unprecedented 10 mas (1 σ) attitude determination accuracy at a 5 Hz rate. The approach developed at NRL to accomplish this objective is presented.

JMAPS Fine Attitude Determination: Instrument fine attitude determination starts with the current spacecraft attitude estimates determined by the Kalman filter that combines star tracker and gyro measurements and estimates the attitude at 5 as (1 σ) accuracy. Using the spacecraft attitude and the onboard star catalog, guide stars in the instrument field of view (FOV) are identified. Guide star windows are then placed around the expected star locations as shown in Fig. 2. Typically, a 64 pixel by 64 pixel guide star window will be placed for an initial acquisition. The size of the guide star window decreases as the instrument fine attitude becomes available. Fine attitude determination is performed by comparing the measured centroid locations of the guide stars to their expected locations at the centers of the windows.

Thanks to the small size of the guide star window, which is less than 64 pixels or 32 as, the process of refining attitude estimates through the instrument measurements is considered a small angle attitude update with respect to a reference attitude. This permits application of small angle attitude determination methods in addition to well-known, general-purpose algorithms such as TRIAD, QUEST, and q-method.[2] Using the small angle assumption, a new computationally efficient algorithm[3] was developed based on the homogeneous transformation (HT) that has typically been used to describe robot manipulator kinematics.

Simulations and Results: The performance of the HT algorithm is evaluated and compared to well-known algorithms TRIAD, q-method, and QUEST. Only two guide stars are employed to compare the HT algorithm against the TRIAD algorithm since it (TRIAD) is limited to operating on two stars at a time. Ten guide stars are used to evaluate the HT algorithm in comparison to q-method and QUEST. Focal plane star images are simulated with random centroiding errors as well as attitude biases and the algorithms are applied to estimate the attitude correction. As an example of the results, Fig. 3 shows the cross-boresight axis accuracy, defined as the standard deviation of 500 attitude estimates subtracted from the truth value. Standard deviations are shown for 20 different guide star patterns within the FOV. The left-hand plot in Fig. 3 shows the results among q-method, QUEST, and HT algorithms using 10 guide stars, while the right-hand plot reflects the comparison between TRIAD and HT algorithms using two guide stars only. All methods produce similar results for 10 guide stars and the HT algorithm performs better with two guide stars against TRIAD. Attitude estimation errors decrease with a larger number of guide stars.

Summary: Simulations establish that the unprecedented goal of 10 mas (1 σ) attitude determination accuracy can be met with the JMAPS instrument and

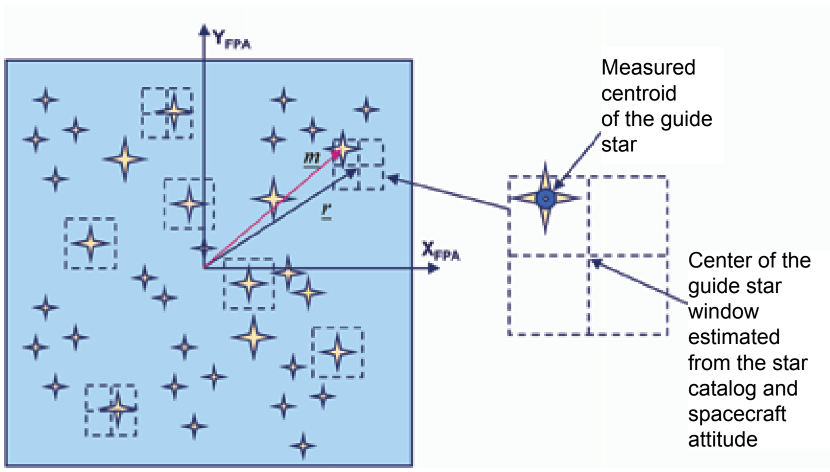

FIGURE 2
Guide stars and their windows in the focal plane array (FPA).

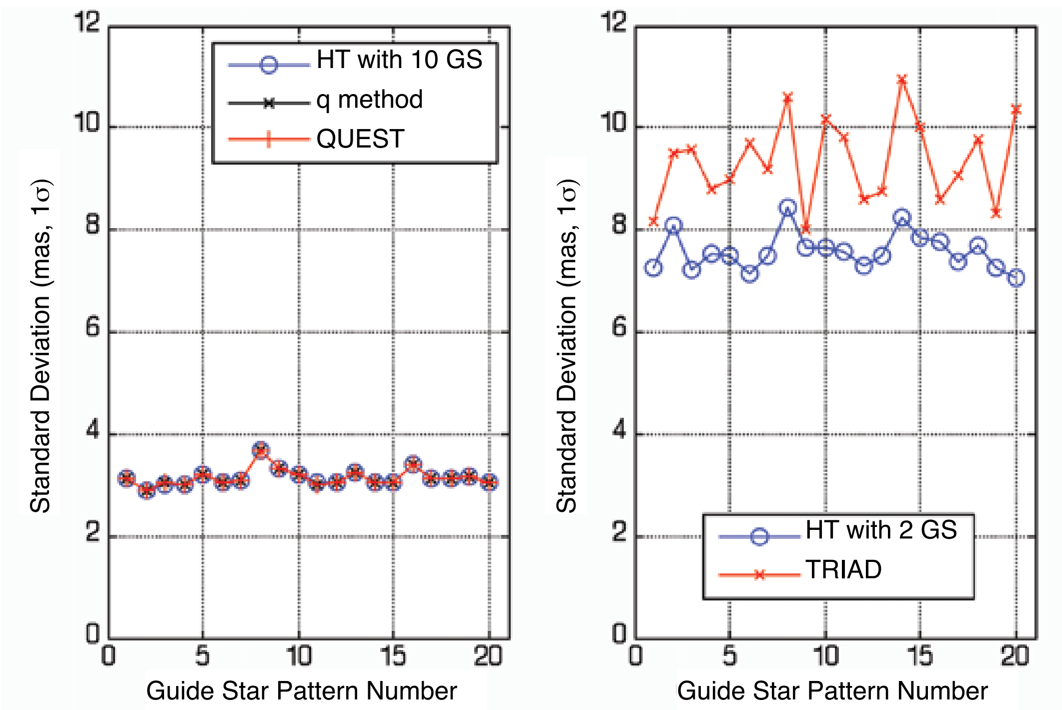

FIGURE 3
Standard deviation of cross-boresight attitude error estimates with 10 guide stars (left) and with 2 guide stars (right).

various attitude determination algorithms. In particular, the HT algorithm provides attitude determination accuracy comparable to the existing TRIAD, q-method, and QUEST algorithms while requiring less than half the computation cost of the other methods. The HT algorithm can produce attitude estimates when at least two guide stars are available and take as many as available guide stars in the instrument FOV, offering flexibility with instrument operation as a star tracker.

[Sponsored by ONR]

References

[1] B.N. Dorland, R.P. Dudik, Z. Dugan, and G.S. Hennessy, "The Joint Milli-Arcsecond Pathfinder Survey (JMAPS): Mission Overview and Attitude Sensing Applications," AAS Paper 09-181, 19th AAS/AIAA Space Flight Mechanics Meeting, Savannah, GA, Feb. 9–12, 2009.

[2] M.D. Shuster and S.D. Oh, "Three-Axis Attitude Determination from Vector Observations," *J. Guidance, Control and Dynamics* **4**(1), 70–77 (1981).

[3] T.W. Lim, F.A. Tasker, and P.G. DeLaHunt, "The Joint Milli-Arcsecond Pathfinder Survey (JMAPS) Instrument Fine Attitude Determination Approach," AAS Paper 10-031, 33rd AAS Guidance and Control Conference, Breckenridge, CO, Feb. 2010.

TacSat-4, Advanced UHF SATCOM

M. Hurley,[1] W. Raynor,[1] M. Johnson,[1] K. Weldy,[1] E. Becker,[1] C. Amend,[1] M. Nurnberger,[1] T. Duffey,[1] R. Skalitzky,[1] T. Specht,[1] E. Bradley,[1] R. Baldauff,[1] J. Arminger,[1] J. Barnds,[1] K. Akins,[1] J. Hicks,[1] E. Sydow,[1] G. Sandhoo,[1] D. Bentz,[2] B. Davis,[3] and E. Gruner[3]
[1]*Spacecraft Engineering Department*
[2]*Harris Corp.*
[3]*Space-Ground System Solutions*

Mission Summary and Status: TacSat-4 is a Navy-led joint mission[1] to augment current satellite communications (SATCOM) capabilities and to advance Operationally Responsive Space (ORS) systems. The TacSat-4 mission was selected by a joint process culminating in a flag and general officer vote by Army, Navy, Air Force, Marine Corps, and U.S. Strategic Command. TacSat-4 provides 10 ultra high frequency (UHF) channels, which can be used for any combination of communications, data exfiltration, or Blue Force Tracking (BFT). TacSat-4's unique orbit augments geosynchronous SATCOM by providing near-global, but not continuous, coverage including the high latitudes. TacSat-4 improves on current SATCOM by providing communications-on-the-move for existing radios without requiring antenna pointing. TacSat-4 provides flexible up and down channel assignments, which increases the ability to operate in some interfered environments. The Virtual Mission Operations Center (VMOC) tasking system coupled with the orbit allows dynamic reallocation, within 24 hours during normal operations, to different theaters worldwide, enabling rapid SATCOM augmentation when unexpected operations or natural events occur.

FIGURE 4
TacSat-4 during bus-to-payload mating.

In October 2009, NRL engineers completed the spacecraft (see Fig. 4). TacSat-4 is awaiting launch in the fall of 2010 on a Minotaur-IV launch vehicle from Kodiak, Alaska. If military utility is confirmed during the first year of flight operations, TacSat-4 flight operations will be extended for at least 2 more years, and a follow-on acquisition of one to four spacecraft will be considered to augment existing UHF SATCOM. A constellation of four spacecraft provides three or more theaters with 24/7 coverage.

NRL is the program manager, with the Office of Naval Research funding the payload, management, and first year of operations as the lead sponsor. The Office of the Secretary of Defense Office for Technology/Director of Defense Research and Engineering funded the standardized spacecraft bus. The Operationally Responsive Space Office and Air Force's Space and Missile Systems Center (SMC) are providing the launch on a Minotaur-IV. NRL's Blossom Point Ground Station will perform operations in coordination with Naval Network Warfare Command and the Global and Regional SATCOM Centers.

Enabling Technologies: Multiple technologies were used to provide this capability on a small satellite (less than 500 kg) and to provide users straightforward access to the flexible UHF SATCOM "COMMx" payload with dynamic tasking. The spacecraft is shown in Fig. 5 with the COMMx payload and spacecraft bus clearly labeled. Technologies of note include the 12-ft deployable payload antenna, the payload's thermal subsystem, a standardized spacecraft bus, and the Virtual Mission Operations Center.

Enabling Technology — Payload Antenna: The most visible and one of the most challenging subsystems was the 3-m (12-ft) diameter payload antenna. This UHF antenna operates over a frequency range of 240 to 420 MHz. Challenging requirements on the antenna included a 60 lb mass allocation, stowed mode of greater than 60 Hz and deployed mode at greater than 5 Hz, ability to withstand 1 MRad of total ionized dose (TID) radiation, a temperature range of ±150 °C, and low passive intermodulation (PIM). PIM is generated by loose or "dirty" metal-to-metal contacts in the RF field. If PIM were to occur, it effectively raises

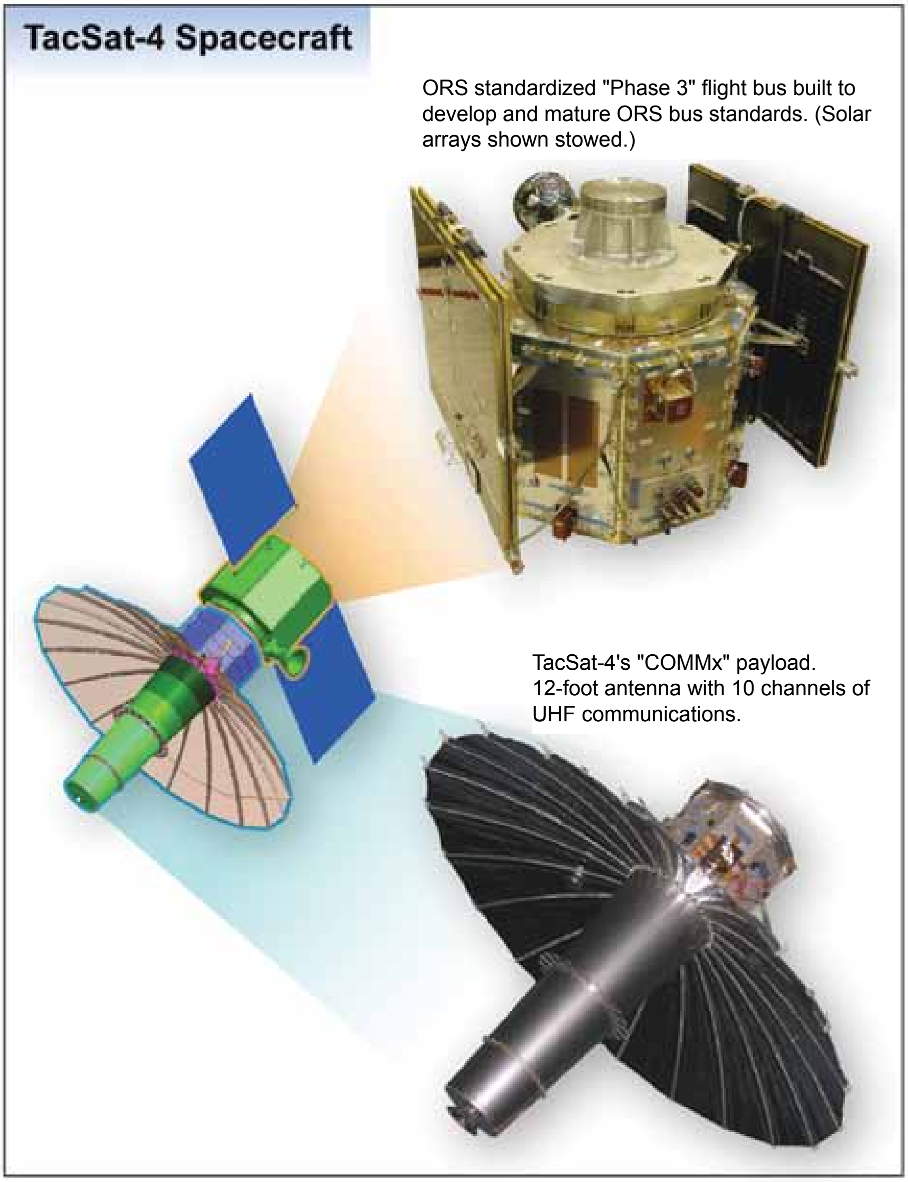

FIGURE 5
The TacSat-4 spacecraft.

the noise floor of an antenna, quickly reducing the performance to unacceptable levels for a system with multiple simultaneous channels (TacSat-4 has 10 channels). The antenna design took advantage of relatively loose surface “flatness” requirements and used a novel Kapton®-Copper flex circuit for the reflector material, as well as several capacitive coupling techniques. The detailed design and test results are documented in Ref. 2.

Enabling Technology — Thermal Subsystem: The challenges facing the COMMx Thermal Control System (TCS) were extensive, most notably the heat dissipation of 600 W within the small payload volume of approximately 1 m diameter by 1 m high. To support TacSat-4’s performance, mass, volume, and integration requirements, a Central Thermal Bus (CTB) design was implemented. The essence of the CTB approach is to package all heat-dissipating devices close to each other at a central location inside the spacecraft while using a cooling technology to (a) collect the waste heat, (b) transport it to the spacecraft radiators, and (c) reject it to space at a place where heat removal is the most efficient (i.e., the coldest sink). The CTB uses both constant conductance heat pipes (CCHP) and loop heat pipe (LHP) technology in conjunction with an LHP temperature control method and thermal diode designs. The TacSat-4 implementation has proven the design through testing and model comparisons. Once launched, this thermal design will be one of the most advanced thermal systems on-orbit. Several papers[3,4] provide design-level detail about this thermal system.

Enabling Technology — Standardized Spacecraft Bus: The TacSat-4 program was also used as a pathfinder to develop and test new spacecraft bus standards for the DoD. NRL and the Johns Hopkins University (JHU) Applied Physics Laboratory (APL) collaborated with an industry team of more than 10 companies to develop, mature, and document standards for small spacecraft systems. The spacecraft bus was built by NRL and APL to mature ORS bus standards developed by an Integrated (government and industry) System Engineering Team, the "ISET Team," with active representation from AeroAstro, Air Force Research Laboratory, APL, ATK Space, Ball, Boeing, Design Net Engineering, General Dynamics AIS, Microcosm, Microsat Systems Inc., Massachusetts Institute of Technology Lincoln Laboratory, Orbital Sciences, NRL, SMC, Space System Loral, and Raytheon. Reference 5 discusses the approach used, including how performance thresholds were established, the iterative application, and maturation of those standards through building the flight bus.

Enabling Technology — Virtual Mission Operations Center: The VMOC is an automated mission operations center that increases user access for tasking requests, STRATCOM apportionment changes (i.e., user priority changes), and dynamic payload capability management. The VMOC leverages the latest web technologies to provide these capabilities. VMOC has been developed and demonstrated since 2003 and is currently moving into an operations mode on the SIPRNET, supporting both TacSat-4 and ORS-1. VMOC is now the baseline tool for payload tasking and asset visibility of all ORS spacecraft.[6]

Conclusion: NRL and our partners have overcome many technical challenges to enable TacSat-4's advanced SATCOM capabilities for the Navy and DoD. TacSat-4 is now complete and awaits launch in late 2010.

[Sponsored by ONR]

References

[1] K. Weldy, A. Hurley, C. Amend, E. Becker, M. Nurnberger, K. Akins, C. Ford, M. Johnson, W. Raynor, and M. Hurley, "TacSat-4 Mission and the Implementation of Bus Standards," Proceedings of the 22nd Annual AIAA Utah State Small Satellite Conference, Logan, UT, Aug. 11–14, 2008, SSC08-III-2.

[2] C. Amend, M. Nurnberger, P. Oppenheimer, S. Koss, and B. Purdy, "A Novel Approach for a Low-Cost Deployable Antenna," Proceedings of the 40th Aerospace Mechanisms Symposium, NASA Kennedy Space Center, FL, May 12–14, 2010, NASA/CP-2010-216272.

[3] R.W. Baldauff, W.J. Arminger, and T.T. Hoang, "Design and Analysis of the Thermal Control System for the TacSat-4 Spacecraft COMMx Payload," *2009 NRL Review,* pp. 114–124.

[4] R. Baldauff, W. Arminger, and T. Hoang, "Design and Analysis of the Thermal Control System for the TacSat-4 Spacecraft, COMMx Payload," Aerospace International Two Phase Conference, Oct. 2009 (this paper includes more detailed presentation and figures of the thermal system).

[5] G. Sandhoo, A. Rogers, P. Stadter, E. Finnegan, M. Hurley, M. Johnson, W. Raynor, P. Schwartz, and J. Griswold, "Standards for Responsive Small Satellites," European Space Agency 4S Symposium, Small Satellites Systems and Services, Rhodes, Greece, 26–30 May 2008.

[6] E. Miller, O. Medina, M. Hurley, and J. Barlow, "Virtual Mission Operations Center and the ORS Ground System Enterprise," AIAA-RS7-2009-6001, AIAA 7th Responsive Space Conference, Los Angeles, CA, April 27–30, 2009.

Integrating the Sun-Earth System for the Operational Environment (ISES-OE)

J.L. Lean,[1] J.D. Huba,[2] S.E. McDonald,[1] S. Slinker,[2] D.P. Drob,[1] J.T. Emmert,[1] R.R. Meier,[1] J.M. Picone,[1] G. Joyce,[2] J. Krall,[2] A. Stephan,[1] K.A. Roach,[1] H. Knight,[1] S.P. Plunkett,[1] C.-C. Wu,[1] B.E. Wood,[1] Y.-M. Wang,[1] R.A. Howard,[1] J. Chen,[2] P.A. Bernhardt,[2] and J.A. Fedder[3]
[1]*Space Science Division*
[2]*Plasma Physics Division*
[3]*Icarus Research, Inc.*

Introduction: NRL's Space Science and Plasma Physics Divisions have commenced an ambitious joint venture: Integrating the Sun-Earth System for the Operational Environment (ISES-OE). The primary goal of this program is to quantitatively understand the space environment above 100 km altitude. This highly variable region can impact Naval operations by disrupting communications and navigation. Central to the ISES effort is an ensemble of multiyear simulations with Sun-Earth system models that calculate ionospheric composition,[1] neutral composition,[2] and winds,[3] along with electrodynamical integration of the surrounding space plasma.[4] ISES-OE uses additional NRL models and observations of solar extreme ultraviolet (EUV from 0 to 120 nm) spectral irradiance,[5] ambient solar wind,[6] and coronal mass ejections.[7] Large databases of drag-derived and remotely sensed neutral thermospheric densities constructed with NRL algorithms[8] and GPS-derived total electron content (TEC) are being analyzed to provide model validation on time scales as long as the 11-year solar cycle. Figure 6 sketches the ISES components.

An Expanded Operational Domain — the Sun-Earth System: Accompanying the expansion of Naval

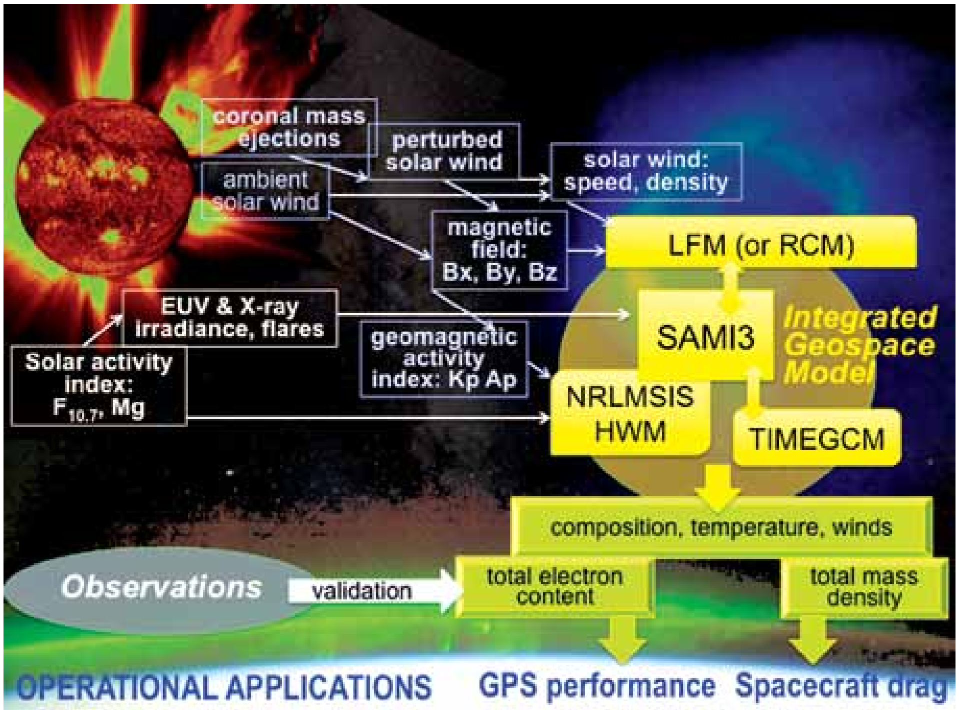

FIGURE 6
In this schematic of ISES program elements, the components of the integrated geospace model are identified in yellow, with the SAMI3 ionospheric model (along with the NRLMSIS and HWM empirical models) at the core. Physical integration is underway with TIMEGCM, RCM, and LFM to physically couple the thermosphere, plasmasphere, and magnetosphere, respectively. Drivers of geospace fluctuations occur in two primary forms, via solar EUV photons (orange) and particles and plasma in the solar wind (purple). Observations of ionized and neutral densities in the thermosphere and ionosphere provide model validation.

activities beyond the surface of the Earth is a growing awareness of adverse space environment impacts on sophisticated military systems. Earth-orbiting spacecraft support myriad Fleet operations for which command, control, communications, and computer systems (C4) are crucial. Charged particles in the F layer (200 to 400 km) transmit, reflect, retard, and refract kHz to MHz radio waves that enable C4 capabilities. Neutral gases impede the motion of the more than 15,000 Earth-orbiting objects that the U.S. Space Command tracks. Because the space environment fluctuates widely, robust knowledge of geospace fosters tactical advantage in Naval operations by reducing uncertainties in communications and navigation, radar accuracy, targeting precision, orbit prediction, and space situational awareness.

The Changing Ionosphere and Atmosphere: Charged and neutral densities in the F region can increase by an order of magnitude or more in response to changing solar activity. From the minimum to maximum of the Sun's 11-year activity cycle, TEC increases from ~10 to more than 40 TECU (1 TECU = 10^{16} electrons per m^2). Correspondingly, the maximum reflected radio frequency increases from 3 to 12 MHz. Figure 7 illustrates the changes of 5 to 10 TECU in global TEC as a result of changing irradiance (as the Sun rotates on its axis over 27 days), and of annual and semiannual oscillations (AO and SAO). Regional fluctuations can exceed the global changes by an order of magnitude. The geographical maps in Fig. 8 illustrate how the local TEC maximum tracks the subsolar point throughout the day, with subequatorial enhancements (the equatorial anomaly) resulting from electrodynamics and winds.

Integrated Geospace Models: The enormity of geospace (a volume four orders of magnitude larger than the Navy's terrestrial operating environment) precludes adequate observational specification. The needed space-based measurements are sparse and intermittent. Global coverage is attainable only with numerical models, but integrated geospace models are in their infancy. Simulations that integrate the thermosphere, ionosphere, plasmasphere, and magnetosphere began only in 2001, three decades after numerical models of terrestrial weather integrated the lower atmosphere, oceans, and land.

Because electron, ion, and neutral particle variations in the ionosphere and thermosphere (from ~90 to 600 km) are the prime source of space impacts on the operational environment, the core of the ISES integrated model is NRL's state-of-the-art ionospheric model, SAMI3,[1,4] and its embedded thermosphere. Unique among ionospheric models for its numerical sophistication, SAMI3 solves continuity and momentum equations for seven ion species on a non-orthogonal, non-uniform, single mesh fixed grid that extends to ~8 Earth radii (R_E). The model, which includes a dynamo electric field and accounts for collisionless plasma processes above 2000 km, couples electrodynamically with the surrounding plasmasphere and magnetosphere.[4]

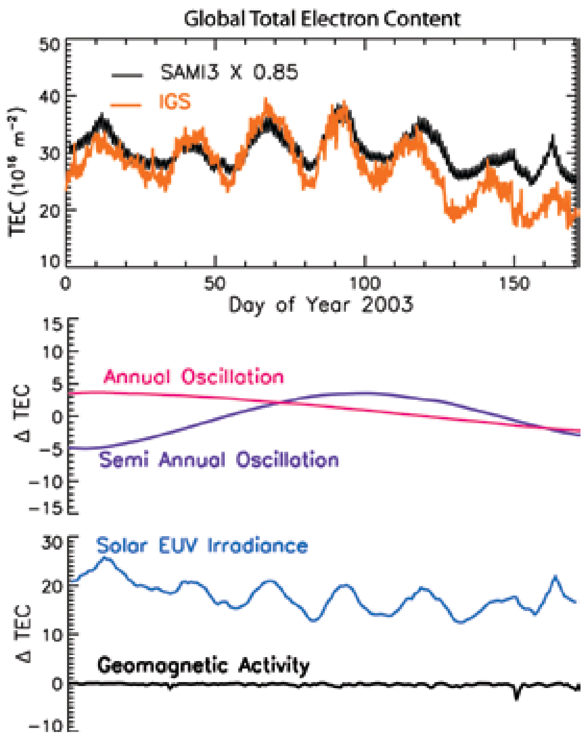

FIGURE 7
Shown are 2-hourly values of global ionsopheric total electron content (TEC) during the first six months of 2003, derived from GPS observations by the International GPS Service (IGS) and simulated with the baseline ISES model. Also shown (in the middle panel) are the changes attributable to the semi-annual and annual oscillations, and (in the lower panel) the solar and geomagnetic activity.

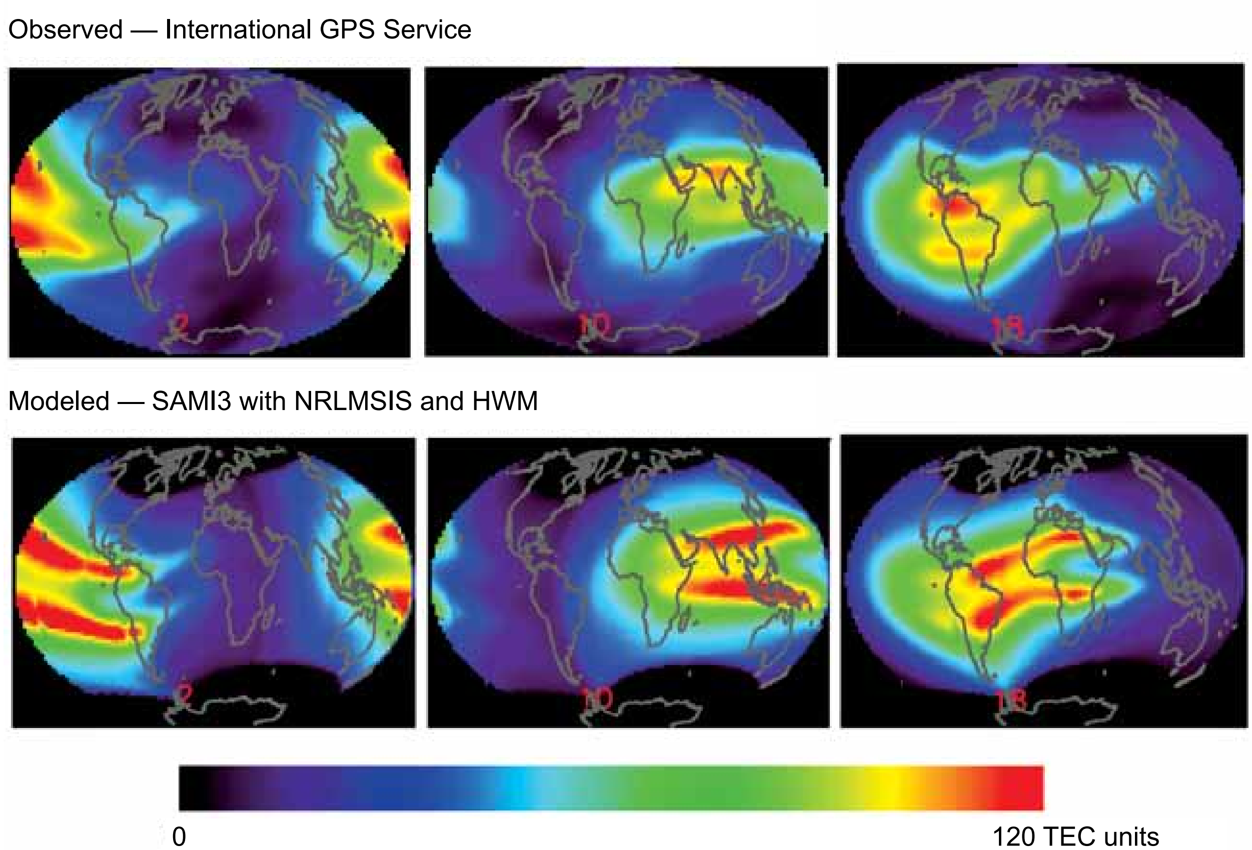

FIGURE 8
Ionospheric total electron content, 31 March 2003. The diurnally driven variations in ionospheric electron content at 2, 10, and 18 hours UT (near midnight, noon, and dusk at 0° longitude) are shown from observations in the upper panel, and simulated by SAMI3 in the lower panel. There are distinct differences in the observed and modeled equatorial anomaly, identified as the high ridges on either side of the magnetic equator.

Model Simulations and Validation: The ISES program expands integrated Sun-Earth system modeling beyond the current community focus on severe, transient geomagnetic storms. ISES also addresses the more persistent and dominant influences of solar irradiance variations changes and the AO and SAO. Underway are simulations of the entire descending phase of solar cycle 23 (i.e., from 2002 to 2008) using a range of model configurations with measured and modeled solar-heliospheric drivers (Fig. 6).

Initial comparisons (Fig. 7) between observed and modeled TEC suggest that modeled TEC are overall higher with weaker monthly and seasonal variations. Probable explanations are that the adopted solar EUV irradiances are too high, and that the AO and SAO in neutral densities are not adequately predicted. The differences (Fig. 8) in the regional structure of the equatorial anomaly likely relate to the model's lack of electrodynamic integration with the surrounding thermosphere and plasmasphere. Future simulations will use a more advanced ISES model in which SAMI3 is integrated with first-principles simulations of the thermosphere (TIMEGCM), the plasmasphere (RCM), and the magnetosphere (LFM). Ultimately, the ISES-OE program will produce a fully integrated and validated geospace model for further exploration and quantification of the complex operational space environment.

[Sponsored by ONR and NASA]

References

[1] J.D. Huba, G. Joyce, and J.A. Fedder, "Sami2 is Another Model of the Ionosphere (SAMI2): A New Low-latitude Ionosphere Model," *J. Geophys. Res.* **105**(A10), 23,035–23,054 (2000).

[2] J.M. Picone, A.E. Hedin, D.P. Drob, and A.C. Aikin, "NRLMSISE-00 Empirical Model of the Atmosphere: Statistical Comparisons and Scientific Issues," *J. Geophys. Res.* **107**(A12), 1468 (2002), doi:10.1029/2002JA009430.

[3] D.P. Drob, J.T. Emmert, G. Crowley, J.M. Picone, G.G. Shepherd, W. Skinner, P. Hays, R.J. Niciejewski, M. Larsen, C.Y. She, J.W. Meriwether, G. Hernandez, M.J. Jarvis, D.P. Sipler, C.A. Tepley, M.S. O'Brien, J.R. Bowman, Q. Wu, Y. Murayama, S. Kawamura, I.M. Reid, and R.A. Vincent, "An Empirical Model of the Earth's Horizontal Wind Fields: HWM07," *J. Geophys. Res.* **113**, A12304 (2008), doi:10.1029/2008JA013668.

[4] J.D. Huba, G. Joyce, S. Sazykin, R. Wolf, and R. Spiro, "Simulation Study of Penetration Electric Field Effects on the Low- to Mid-latitude Ionosphere," *Geophys. Research Lett.* **32**, L23101 (2005), doi:10.1029/2005GL024162.

[5] J.L. Lean and T.N. Woods, "Solar Spectral Irradiance: Measurements and Models," in *Evolving Solar Activity and the Climates of Space and Earth*, eds. C.J. Schrijver and G.L. Siscoe (Cambridge Univ. Press, 2010), pp. 269–298.

[6] Y.M. Wang, N.R. Sheeley, Jr., J.L. Phillips, and B.E. Goldstein, "Solar Wind Stream Interactions and the Wind Speed-Expansion Factor Relationship," *Astrophys. J.* **488**, L51 (1997).

[7] R.A. Howard, J.D. Moses, A. Vourlidas, J.S. Newmark, D.G. Socker, S.P. Plunkett, C.M. Korendyke, J.W. Cook, A. Hurley, and J.M. Davila, "Sun Earth Connection Coronal and Heliospheric Investigation (SECCHI)," *Space Science Reviews* **136**(1-4), 67–115 (2008).

[8] J.T. Emmert, R.R. Meier, J.M. Picone, J.L. Lean, and A.B. Christensen, "Thermospheric Density 2002–2004: TIMED/GUVI Dayside Limb Observations and Satellite Drag," *J. Geophys. Res.* **111**, A10S16 (2006), doi:10.1029/2005JA011495.

Origins of Solar Energetic Particle (SEP) Variability

Y.-K. Ko and A.J. Tylka
Space Science Division

The SEP Radiation Hazard: Solar energetic particle (SEP) events are significant natural radiation hazards for Navy and DoD space-based assets. These episodic outbursts of high-energy protons and ions from the Sun damage solar panels, interfere with sensors, and cause a variety of single-event-effects (SEEs) in spacecraft electronics. Unless vulnerable systems are safe-moded prior to the event, these effects can interrupt or degrade performance not only during an event, but also for an extended period of time after the SEP event is over. Unlike other components of the natural space-radiation environment, SEPs are highly variable in intensity, duration, the distribution of particle energies, and ionic composition.[1] These variable factors, in turn, determine the nature of the radiation hazard posed to satellite systems. Discovering and modeling the factors that drive this variability is the prime objective of SEP research at NRL, with the ultimate goal of a physics-based predictive model of the SEP radiation hazard that can be employed by satellite operators.

SEPs and Fast CMEs: An extensive body of evidence indicates that large SEP events are produced by very fast coronal mass ejections (CMEs), which explode outward from the Sun at speeds exceeding 1000 km/s. As illustrated in Fig. 9, these very fast CMEs drive shocks through the corona and interplanetary medium. Interactions between the shock and suprathermal seed particles produce the high-energy SEPs that endanger spacecraft. In particular, the shock expands and crosses many magnetic field lines, which emerge from different source regions on the Sun. Since the SEPs are charged particles, they travel outward along the magnetic field lines, provided that cross-field diffusion is small. Thus, the SEPs subsequently observed at Earth should retain some signature of the source regions from which the magnetic field lines and the seed particles emerged.

SEPs and Source Regions: We have recently discovered evidence that ties SEP compositional variability to specific structures on the solar surface.[2] By employing heliospheric magnetic-field mapping techniques developed by NRL Space Science Division scientists,[3] we first traced the solar wind magnetic field lines that guide the SEPs from Sun to Earth back to their origination point at the Sun. We then used data from NASA's Wind and ACE spacecrafts to analyze the elemental composition of SEPs and the solar wind.

Figure 10 shows the synoptic Carrington maps of the Sun for eight SEP events from 2004 to 2006. Marked on each are the source location of the CME that produced the SEP event and the footpoint of the magnetic field line that connected the Sun to Earth at the time of the SEP event. In the four examples at the left, this footpoint is from a coronal hole (CH); in the four examples on the right, this footpoint is from an active region (AR). A "coronal hole" is a structure on the solar surface that appears as a dark patch in the extreme ultraviolet (EUV) or X-ray image of the Sun. An "active region" is another structure on the Sun with bright magnetic loops when seen in EUV and X-rays, and with strong underlying magnetic field. The solar wind, which carries open magnetic field lines from the Sun out into the heliosphere, can originate from either coronal holes or active regions.

The left panel of Fig. 11 shows hourly averaged iron-to-oxygen (Fe/O) ratios at 5 to 10 MeV/nucleon from these and four other SEP events in 2004 to 2006, correlated against the Fe/O measured simultaneously in the thermal solar wind. (Fe/O provides a particularly sensitive measure of heavy-ion variability in SEPs and the solar wind.) In the correlation plot, data points associated with AR sources are displayed as red symbols; data points associated with CH sources are black.

The right panels of Fig. 11 show the histograms generated from these data, color coded as before. Although the SEP distributions are by no means bimodal, a larger SEP Fe/O preferentially appears when the footpoint is from an AR, and a smaller SEP Fe/O preferentially appears when the footpoint is from a CH. In contrast, the solar-wind particles that emerge from ARs and CHs have almost identical Fe/O distributions.

Implications: These results are the first successful example of tracking SEP compositional variation back to differences in the source of the guiding magnetic field. These results indicate that near-real-time mapping of the interplanetary magnetic field from Earth to its solar-source structure may provide a means of forecasting the heavy-ion content of SEP events, a particularly important concern for SEEs. New puzzles are the processes that cause the compositional difference between SEPs and the solar wind, and why these processes are different for active regions and coronal holes. Thus, this discovery provides not only a new window on SEP variability, but also on the physics of solar regions that give rise to the solar wind.

[Sponsored by ONR]

References

[1] A.J. Tylka and M.A. Lee, "A Model for Spectral and Compositional Variability at High Energies in Large, Gradual Solar Particle Events," *Astrophys. J.* **646**, 1319–1334 (2006).

[2] Y.-K. Ko, A.J. Tylka, C.K. Ng, and Y.-M. Wang, "Solar Wind Source Regions and Variability in Heavy-Ion Composition in Gradual Solar Energetic Particle Events," submitted to *Astrophys. J.*, 2010.

[3] Y.-M. Wang, M. Pick, and G.M. Mason, "Coronal Holes, Jets, and the Origin of ^{3}He-rich Particle Events," *Astrophys. J.* **639**, 495–509 (2006).

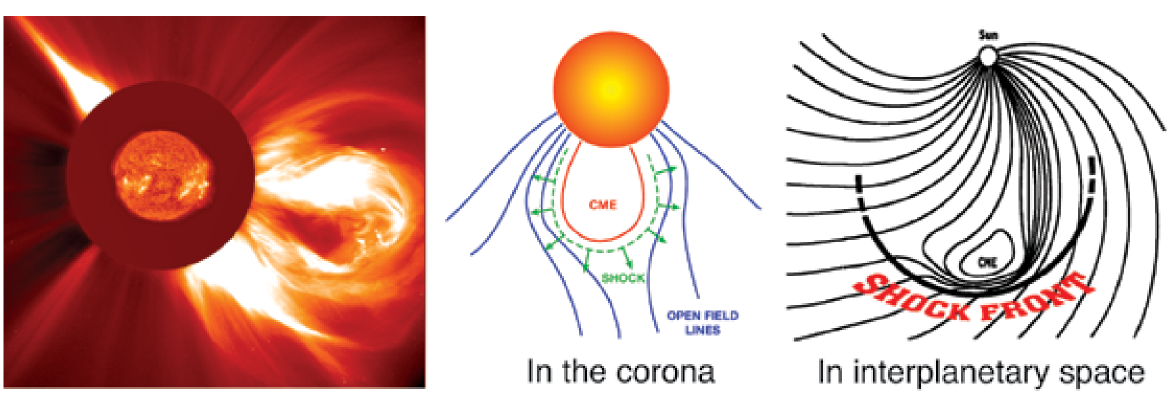

FIGURE 9

(Left) A coronal mass ejection, as imaged from the Sun-Earth L1 Lagrangian point by NRL's Large Angle and Spectrometric Coronagraph (LASCO) aboard the Solar and Heliospheric Observatory (SOHO) spacecraft. Two cartoons of the CME and the CME-driven shock, as viewed from above the ecliptic plane, while in the corona (center) and in interplanetary space (right), moving through the heliospheric magnetic field.

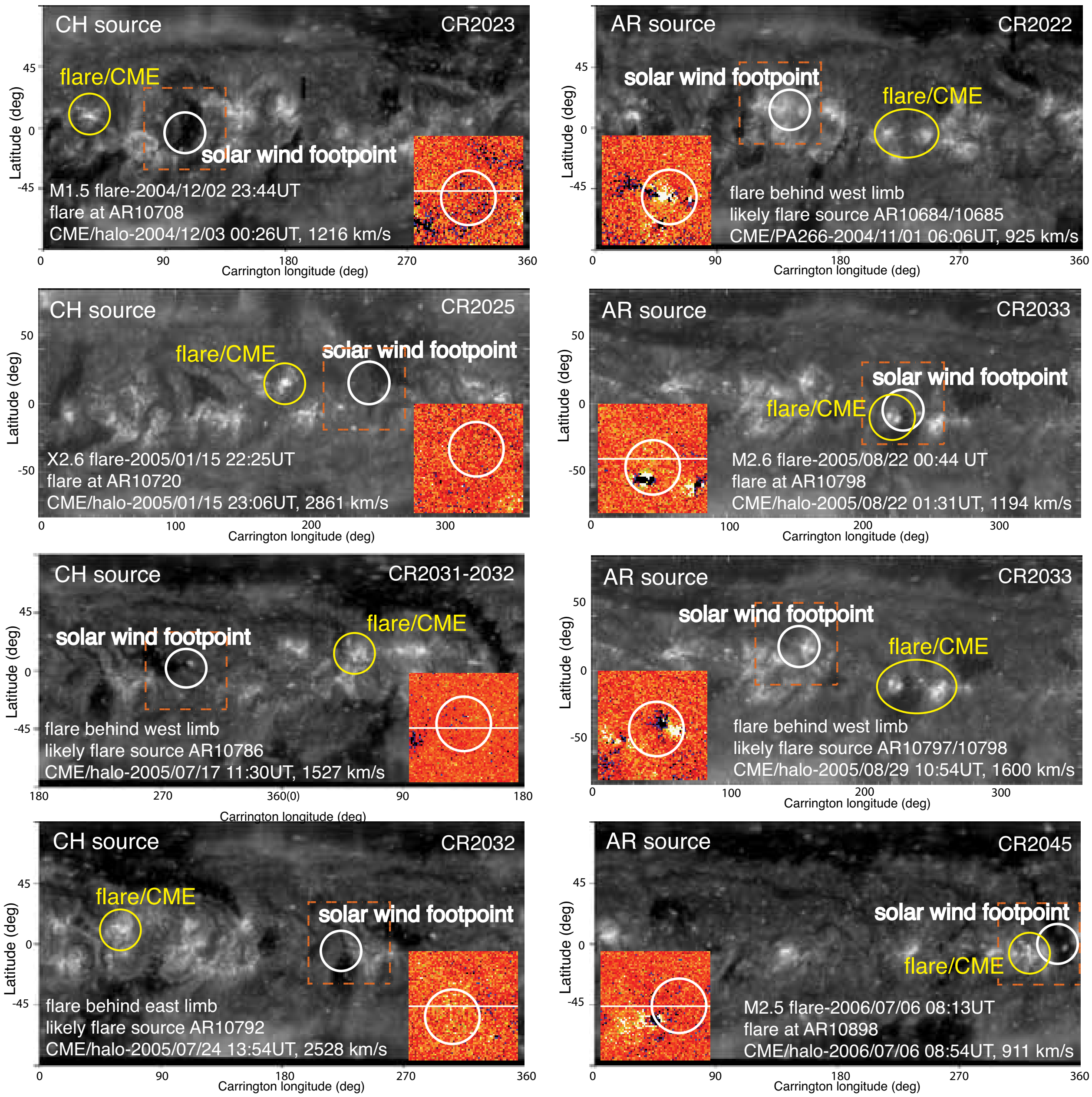

FIGURE 10
Carrington maps for eight SEP events, with the eruption point of the CME and the footpoint of the Sun-Earth magnetic field line marked for coronal-hole (left) and active-region (right) sources. The Carrington maps are constructed from images taken by the NRL-participating Extreme Ultraviolet Imaging Telescope (EIT) aboard SOHO. The insets are corresponding magnetic field synoptic charts (cropped to the same area as the orange-dashed square on the EIT maps, and white/black patches representing positive/negative field) from the Michelson Doppler Imager (MDI) aboard SOHO.

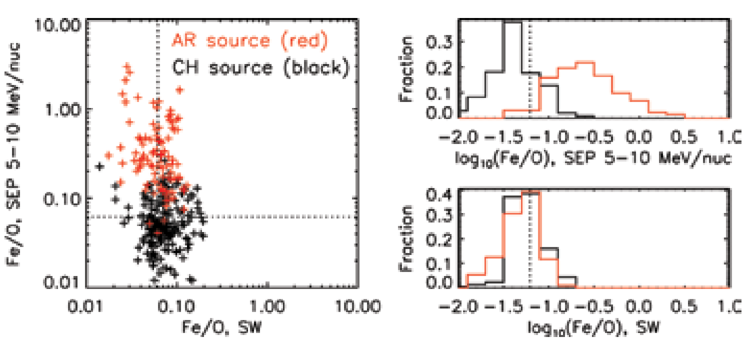

FIGURE 11
(Left) Correlation plot of hourly averaged SEP Fe/O at 5 to 10 MeV/nucleon vs simultaneous measurements of the solar-wind Fe/O, measured by the Wind and ACE spacecraft, respectively, both of which were also at L1. Red points correspond to active-region (AR) sources, black points to coronal-hole (CH) sources. (Right) Histograms of the SEP (top) and solar-wind (bottom) Fe/O, with same color coding.

Technology Development for High Integrity GPS (HiGPS)

O.J. Oaks
Space Systems Development Department

Background: The Naval Research Laboratory is investigating the capability to augment GPS navigation and time synchronization using the existing constellation of Iridium satellites. The technology concept, HiGPS, is based on prior work and demonstrations provided by The Boeing Company. NRL is leveraging experience and expertise gained from the early NRL Timation and Navigation Technology Satellite development programs and more than 30 years experience supporting GPS development and operation to exploit the concept of providing a robust anti-jam capability for navigation and time synchronization. The concept aids GPS in using the Iridium communications satellite signals. NRL has teamed with prime contractor Boeing and subcontractors Iridium, Coherent Navigation, and Rockwell Collins to provide the GPS anti-jam enhancement in the very near future. This requires technology development of a signal-in-space, ground infrastructure, and user equipment that will support the HiGPS augmentation concept. The signal-in-space development leverages on the existing Iridium satellite communication signals and the infrastructure that supports them. The technology development effort is ongoing and several milestone achievements have demonstrated the potential to deliver anti-jam navigation and time synchronization capability in the near future. In June 2008, a successful test was performed at NRL that provided time synchronization to military communications equipment while being jammed, and in June 2009, a successful test was performed at NRL that demonstrated anti-jam capability for navigation. The objective is to develop the anti-jam technology that can be transitioned to operation in 2011.

Iridium is a communications satellite system of 66 space vehicles in low Earth orbit (LEO). The constellation consists of 6 planes of 11 satellites in polar orbits that provide continuous global Earth coverage. Compared with GPS, Iridium has a lower altitude and a higher transmitted power, and therefore provides a significantly stronger received signal that can be exploited for aiding the GPS signals in navigation and time synchronization applications. The Iridium satellite onboard communications electronics is reprogrammable and can be configured to transmit signals that are suitable for navigation and to aid time synchronization. The Iridium ground control is being expanded to support the new signal-in-space that will be delivered to GPS users that have the HiGPS augmentation capability. The objective is to provide Iridium aiding signals in areas where GPS may be denied by interference or jamming. The concept uses ground reference stations outside the area of interference that simultaneously receive Iridium and GPS signals. The reference stations derive data that relate GPS to the Iridium signals and allow precise prediction of the GPS signal. This information is sent as augmentation data to users via the lower-altitude, higher-power Iridium satellites. The users process this information to enable reception of the GPS signals in a high-noise environment. This augmentation capability has the potential to provide more robust navigation and time synchronization, including higher jamming and interference rejection, faster acquisition times, and improved accuracy.

Technology Components and System Concept: The technology system components under development consist of reference stations, the HiGPS designed signal-in-space, the user equipment designed to combine the HiGPS augmentation data with the GPS signals, and an operations center with a ground network connected to the reference stations and Iridium satellite control station. Figure 12 presents a simplified system concept. The first-generation HiGPS signal-in-space that has been deployed is the Enhanced Narrowband signal, so named because it has the same characteristic 40 kHz narrow bandwidth of the Iridium communications signals. The ranging accuracy using this signal is several microseconds because of the narrow bandwidth. A near-term, future-generation Advanced Waveform signal is under development that will have a bandwidth greater than 7 MHz, which will provide a ranging accuracy more like the GPS signal of several nanoseconds. The augmentation data modulated on the HiGPS signal includes the GPS broadcast data, the Iridium satellite ephemerides, and Iridium-to-GPS carrier phase difference data. The HiGPS receivers remove the GPS broadcast data from the received GPS signals, allowing a longer integration time for coherently tracking the GPS carrier signal. The integration time is increased from 20 ms to 5 s, providing a 30 dB improvement in signal-to-noise. Iridium ephemerides are required to perform an initial geolocation using only the Iridium signal. For cold-start acquisition in a GPS-denied environment, the HiGPS receiver must first acquire the Iridium signal, obtain the augmentation data, and compute an initial position using measurements from the Iridium signal. Once the data are obtained and the geolocation is sufficient, the HiGPS receiver can then acquire and track the GPS signals in a high-noise environment. The carrier phase difference data are used to aid the receiver in acquiring and maintaining carrier phase-lock on the GPS signal.

The data are precise to 20 picoseconds, which is a fraction of a carrier cycle and provides submeter

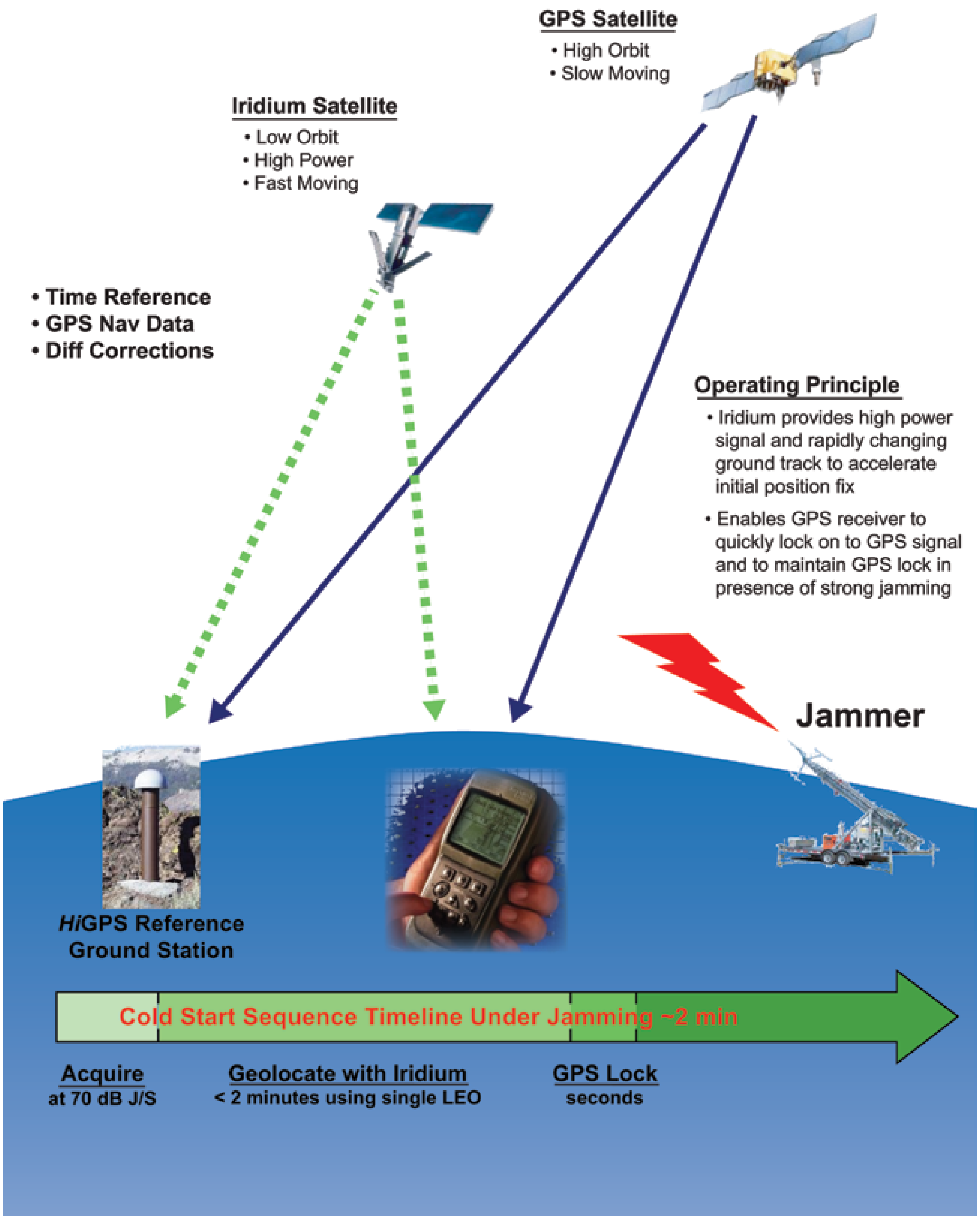

FIGURE 12
HiGPS operational concept.

accuracy in the position solution. A first-generation prototype HiGPS receiver has been completed along with reference stations that have been deployed to support technology demonstrations.

Technology Demonstrations Enabling Use of GPS in a Jammed Environment: An initial tracking demonstration was performed in 2007 that demonstrated the feasibility of the concept. The results achieved greater than 20 dB improvement in anti-jam performance with submeter accuracy in position. In this demonstration, the receiver was already tracking Iridium and GPS before the jamming was turned on and the time of operation was limited to 30 s. Since that time, the HiGPS Program has been further developing the technology to provide acquisition in a jammed environment and more continuous operation across many Iridium satellites. In June 2009, a test was performed at NRL that demonstrated the ability to provide the HiGPS signal over an area of operation and to acquire GPS signals in a jammed environment. Figure 13 is a screen shot of the command console showing deployment of the HiGPS signal over the test area at NRL. The signals were provided over NRL in a matter of seconds after the command was sent. The reference station for the test was in Philadelphia, Pennsylvania, and the operation center was in southern California. The test used the first-generation deployed ground infrastructure network. Figure 14 is a series of pictures that show acquisition of the GPS signals in a jammed environment, which was performed at NRL during the demonstration tests. The focus of the test was on acquisition and not tracking. The acquisition performance achieved an anti-jam improvement greater than 30 dB over the currently fielded GPS receivers with an accuracy of several meters and a time to first GPS determined position of roughly two minutes. This performance will improve as the technology is refined during 2010. The current focus of the HiGPS Program is to merge the tracking capability demonstrated in 2007 with the acquisition capability demonstrated in 2009. The 2010 and 2011 efforts include demonstrating the complete system capability in field tests and initiating a plan to transition the technology to the warfighter.

[Sponsored by ONR]

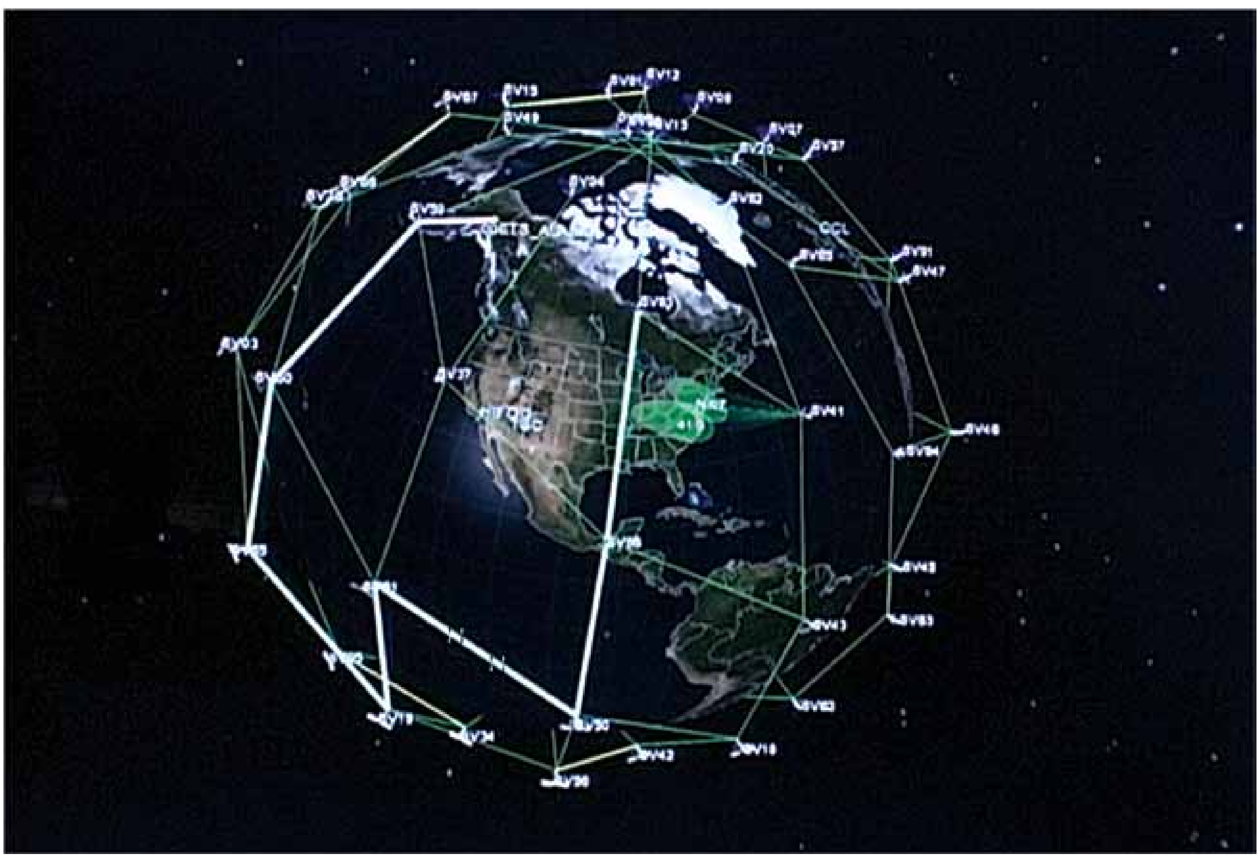

FIGURE 13
The HiGPS signal-in-space is uploaded from Fairbanks, AK, via crosslinks to the Iridium satellite, which provides the signal to the NRL test area within seconds of commanding.

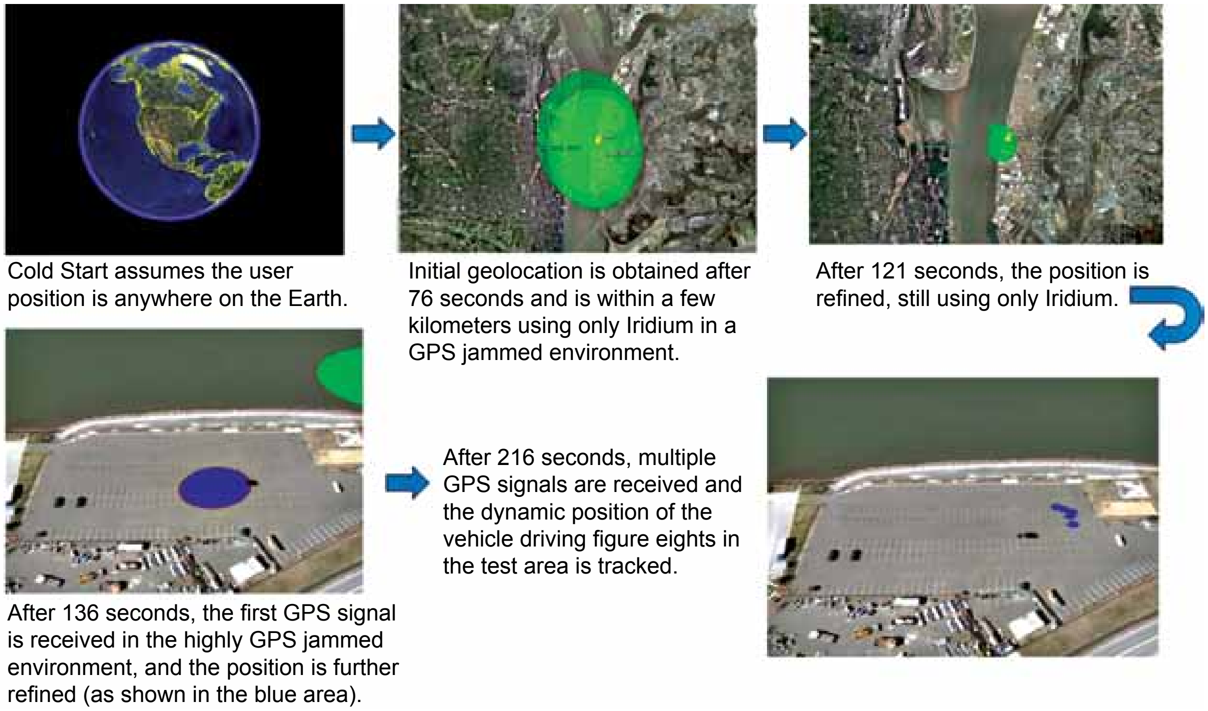

FIGURE 14
Demonstration of GPS acquisition in a jammed environment.